Yohana et al., *Cogent Engineering* (2019), 5: 1562319
https://doi.org/10.1080/23311916.2018.1562319

cogent engineering

MECHANICAL ENGINEERING | RESEARCH ARTICLE

Numerical analysis on the effect of the vortex finder diameter and the length of vortex limiter on the flow field and particle collection in a new cyclone separator

Eflita Yohana[1], Mohammad Tauviqirrahman[1]*, Arbian Ridzka Putra[1], Ade Eva Diana[1] and Kwang-Hwan Choi[2]

Received: 01 June 2018
Accepted: 18 December 2018
First Published: 24 December 2018

*Corresponding author: Mohammad Tauviqirrahman, Department of Mechanical Engineering, Diponegoro University, Jl. Prof. Sudharto, SH., Semarang 50275, Indonesia
E-mail: mohammad.tauviqirrahman@ft.undip.ac.id

Reviewing editor:
Duc Pham, School of Mechanical Engineering, University of Birmingham, UK

Additional information is available at the end of the article

Abstract: There are many geometric and operational parameters that affect the performance of a cyclone separator, including the geometry and the length of the vortex within the cyclone. In this work, a Computational Fluid Dynamics calculation is presented to predict the cyclone performance and flow field of a new cyclone separator. The simulation was realized using Reynolds Stress Model (RSM) for the turbulent model and the Discrete Phase Model (DPM) for particle trajectories. The Rosin–Rammler method is used in numerical simulations to apply Particle Size Distribution (PSD). The velocity fluctuations are simulated using the Discrete Random Walk (DRW) method. Simulation results show that the reduced vortex

ABOUT THE AUTHORS

Eflita Yohana received her Bachelor Engineering degree in Mechanical Engineering from Brawijaya University, Indonesia, her Master Engineering degree in Mechanical Engineering form Gadjah Mada University, Indonesia, and obtained her Doctoral degree from Pukyong National University, South Korea.

Mohammad Tauviqirrahman received his BEng in Mechanical Engineering from University of Diponegoro in 2003, his MEng in Mechanical Engineering from Institute Technology Bandung, and Doctoral in Laboratory for Surface Technology and Tribology, University of Twente, the Netherlands.

Arbian Ridzka Putra received his Bachelor Engineering degree in Mechanical Engineering from Diponegoro University, Indonesia.

Ade Eva Diana received her Bachelor Engineering degree in Mechanical Engineering form Diponegoro University, Indonesia.

Kwang-Hwan Choi is a professor in the Departement of Refrigeration and Air Conditioning Engineering, Pukyong National University, South Korea. He received his Ph.D degree from Waseda University, Japan. His research field are in the areas of desiccant cooling system development by using renewable energy during summer season, especially focusing on solar thermal energy.

PUBLIC INTEREST STATEMENT

The industrial use of separators has become widely used and is continuously being developed to meet the needs of more and more varied products. One commonly used separator is the cylone separator because of its reliability and lack of moving parts. A cyclone separator is a tool that uses vortex separation to remove particulates from air, gas, or liquid stream without using filters. A cyclone performance is a pressure drop and collection efficiency. There are many geometrical and operational parameters which influenced the cyclone performance. The present study was the analysis of the effect of vortex finder diameter and vortex limiter length on flow field and collecting efficiency in a new cyclone separator using CFD method. Numerical results show that the increase in vortex finder diameter and length of the vortex limiter can improve collection efficiency.

finder diameter causes an increase in tangential velocity and collection efficiency but at the cost of pressure drop. It is also found that increasing the length of the vortex limiter will decrease the tangential velocity and decrease the pressure drop but can improve the collection efficiency. Results obtained that geometrical parameter influenced the performance of the new cyclone separator.

Subjects: Mechanical Engineering; Fluid Mechanics; Technology

Keywords: new cyclone separator; collection efficiency; vortex finder; vortex limiter

1. Introduction

A cyclone is one of the most widely used tools for particle separation because of its simple design and low construction and operation costs. The cyclone works by separating the solid particles and gases by utilizing both the centrifugal force and the gravitational force that causes the vortex flow to allow the particles and gases to separate; large particles will drop to the bottom and the air with small particles will rise to the top and exit the cyclone. The factors affecting the rate of entrainment of solids from a fluidized bed dryer named particle size distribution (PSD), terminal velocity, superficial gas velocity, particle density, gas properties, and gas flow regime. Therefore, it is necessary to understand the gas-particle flow and separation characteristics of the cyclone (Alavi, Lay, & Makhmali, 2018).

There are many geometric and operational parameters that influence the separation and performance process of a cyclone, specifically the efficiency of increasing and decreasing the pressure, as well as particle diameter, particle density, cyclone separator dimensions, and the velocity at which particles enter. The cyclone has a flow that is complicated and dynamic. Because of this, an efficient mathematical model is required to provide accurate predictions for efficiency and pressure drop; both for the geometrical design of a cyclone and its operational requirements. Various researchers have developed cyclone models with improved performance by evaluating the effects of geometric and operational parameters by modifying the design of the inlets. Zhao, Su, and Zhang (2006) compared the performance of a conventional single inlet (SI) type cyclone with one having spiral double inlets (DI). Their numerical results show that adding spiral double inlets can improve the symmetry of the gas flow pattern and can increase the efficiency of particle separation. The effect of cone dimensions on cyclone performance is also studied in the literature (Elsayed & Lacor, 2011; Xiang & Lee, 2001; Zhao et al., 2006). The researchers showed that if the cone dimensions were greater than the outlet dimensions, then reducing the cone size would result in higher particle collection efficiency without significantly increasing the pressure. Zhu, Kim, Lee, Park, and Kuhlman (2001), Xiang and Lee (2001), and Lim, Kim, and Lee (2004) found that the double cyclone had a lower decrease in pressure, but did not have higher collection efficiency than a conventional cyclone. The research of Karagoz, Avci, Surmen, and Sendogan (2013) presented a different cyclone design, a new cyclone separator, based on the idea of improving cyclone efficiency by increasing the length of the vortex. The difference lies in the separation chamber consisting of an outer cylinder and a vortex limiter. They conducted experimental tests setting different positions of the vortex limiter and how that relates to cyclone performance.

Numerical simulations of cyclones that were started by Griffith and Boysan (1996) were followed by an emergence of numerical studies using computational, fluid dynamic techniques related to cyclone performance. Cortes and Gil (2007) also conducted a study to model the flow of gases and particles by considering several approximate models for the cyclone separator.

As the numerical investigation has an important role for design optimization, this study is intended to obtain the effects of the geometrical parameter to the performance of the new cyclone separator presented by Karagoz et al. (2013). In the present work, the main focus is to explain the effects of varying vortex finder diameter and vortex limiter length. As a noted this is

different with the work of Safikhani and Mehrabian (2016) which focused on flow field in the new cyclone separator by varying the diameter of the vortex limiter, the position of the vortex limiter, and the length of the vortex finder using computational fluid dynamics. Tangential, axial, and radial velocity profiles and also velocity vector are investigated.

2. Methodology

2.1. General equations

For an incompressible fluid flow, the continuity and momentum equilibrium equations are given as follows (Song et al., 2016):

$$\frac{\partial \rho}{\partial t} + \frac{\partial}{\partial x_i}(\rho u_i) = 0 \tag{1}$$

$$\frac{\partial}{\partial t}(\rho u_i) + \frac{\partial}{\partial x_j} = -\frac{\partial p}{\partial x_i} + \frac{\partial}{\partial x_j}\left[\mu\left(\frac{\partial u_i}{\partial x_j} + \frac{\partial u_j}{\partial x_i}\right)\right] + \frac{\partial}{\partial x_j}\left(-\overline{\rho u_i' u_j'}\right) \tag{2}$$

$$u_i = \bar{u}_i + u_i' \tag{3}$$

where x_i is in the position on the x-axis, x_j is in the position on the y-axis, p is the pressure, ρ is the constant gas density, μ is the viscosity, $-\overline{\rho u_i' u_j'}$ is the *Reynolds stress tensor*, $\bar{u}_i$ is the average speed, and u_i' is the x-axis velocity fluctuation component.

For RSM, the transport equation is written as follows:

$$\frac{\partial}{\partial t}\left(\rho \overline{u_i' u_j'}\right) + \frac{\partial}{\partial x_k}\left(\rho u_k \overline{u_i' u_j'}\right) = D_{T,ij} + P_{ij} + \phi_{ij} + \varepsilon_{ij} + S \tag{4}$$

where the two equations on the left are derivatives with respect to time of the convective transport voltages and related equations, whereas the four equations on the right are:

Turbulent diffusion equation:

$$D_{T,ij} = -\frac{\partial}{\partial x_k}\left[\rho \overline{u_i' u_j' u_k'} + \overline{p\left(\delta_{kj} u_i' + \delta_{ik} u_j'\right)}\right] \tag{5}$$

Stress production equation:

$$P_{ij} = -\rho\left(\overline{u_i' u_k'}\frac{\partial u_j}{\partial x_k} + \overline{u_j' u_k'}\frac{\partial u_j}{\partial x_k}\right) \tag{6}$$

Pressure strain equation:

$$\phi_{ij} = \overline{p\left(\frac{\partial u_i'}{\partial x_j} + \frac{\partial u_j'}{\partial x_i}\right)} \tag{7}$$

Dissipation equation:

$$\varepsilon_{ij} = -2\mu\overline{\frac{\partial u_i'}{\partial x_k}\frac{\partial u_i'}{\partial x_k}} \tag{8}$$

In this study, the *discrete random walk* (DRW) model was used based on the stochastic method to determine the velocity of the fluctuating gas. The values u', v', and w' apply during *the lifetime of the turbulent eddy*, while T_e is a sample assumed to obey the Gaussian probability distribution using the following correlation (Safikhani & Mehrabian, 2016).

$$u_i' = \xi\sqrt{\overline{u_i' u_i'}} \tag{9}$$

where ξ is the random number of normal distribution and the term $\sqrt{\overline{u_i'u_i'}}$ represents the local RMS of the speed fluctuations. The characteristics of the *lifetime of the eddy* are defined as the following given constants (Safikhani & Mehrabian, 2016)

$$T_e = 2T_l \tag{10}$$

where T_l represents the *eddy turnover time* given as $T_e = 0.3\frac{K}{\varepsilon}$ regarding the RSM. Another possible option for random variations of the *lifetime of the eddy* is as follows (Safikhani & Mehrabian, 2016):

$$T_e = -T_l \log r \tag{11}$$

where r is a uniform random number between 0 and 1. Particles are assumed to interact with the fluid fluctuation plane that remains throughout the *lifetime of the eddy*. When the *lifetime of the eddy* is reached, a new value of instantaneous velocity is obtained by entering the new value ξ in Equation (9).

This study used a two-phase flow settlement with the Eulerian-Lagrangian approach to predict particle tracks in the cyclone. The path of particles in a stream is calculated using a *discrete phase model* (DPM) to track individual particles.

$$\frac{dx_p}{dt} = \vec{u}_p \tag{12}$$

$$\frac{d\vec{u}_p}{dt} = F_d(\vec{u} - \vec{u}_p) + \vec{g}_x\frac{\left(\rho_p - \rho\right)}{\rho_p} \tag{13}$$

The velocity of the fluid $\left(\vec{u}\right)$, the velocity of the particle $\left(\vec{u}_p\right)$, x_p is the position of the particle, $\vec{g}_x$is the force of gravity, while ρ and $\rho_p$represent the density of the fluid and the particles, respectively. In Equation (13), the term $F_d(\vec{u} - \vec{u}_p)$ reflects the drag force per unit mass of the particle. F_d given as:

$$F_d = \frac{1}{\tau_p}\frac{(C_d - \mathrm{Re}_p)}{24} \tag{14}$$

where τ_p represents the particle's relaxed time and is given as:

$$\tau_p = \frac{\rho_p d_p^2}{18\mu} \tag{15}$$

The *drag coefficient* (C_d) is the numerical function of the Reynolds particle (Re_p). The number of Reynolds particles is defined as:

$$\mathrm{Re}_p = \rho d_p\frac{\left|\vec{u} - \vec{u}_p\right|}{\mu} \tag{16}$$

The drag coefficient for spherical particles was calculated using a correlation developed by Morsi and Alexander (1972) with values of a_1, a_2, and a_3 derived from the relative number of Reynolds particles (Re_p) defined as:

$$C_d = a_1\frac{a_2}{\mathrm{Re}_p}\frac{a_3}{\mathrm{Re}_p} \tag{17}$$

2.2. CFD model

This study uses the Karagoz design for the new cyclone separator (Karagoz et al., 2013) where the vortex limiter, inner cylinder, and outer cylinder substitute for the cone shape to form a vortex as can be seen in Figure 1. The flow tangentially enters the cyclone and moves in a spiral to the lower part of the cylinder through the outer cylinder, almost without friction on the walls, and then the

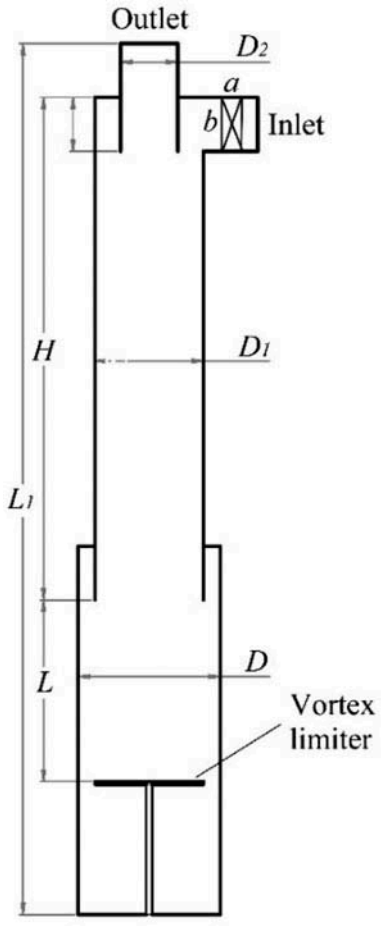

Figure 1. New cyclone separator design.

flow hits the vortex limiter, thereby causing the flow, including the small particles, to move back in opposite directions through the low-pressure, central portion towards the exit of the cyclone. Meanwhile, because of the centrifugal force, the larger particles will be thrown toward the wall and collect in the bottom of the cylinder outside the cyclone. The dimensions of the new cyclone separator dimension in this study are shown in Table 1.

The equations shown in the turbulent models above are numerically resolved using ANSYS Fluid Flow (FLUENT) 16.0. The volume control method is used to discretize the incubative three-dimensional equations of Navier-Stokes. The SIMPLEC scheme is used for pressure-velocity coupling because it is easier to achieve convergence. The selection of the PRESTO scheme for pressure discretization has the

Table 1. Dimensions of the *cyclone* in this study

***Cyclone* Dimension**	**Size (mm)**
Body diameters	D_1 = 190, D = 250
Vortex finder diameter, D_2	80, 100, 120
Inlet section (*a* x *b*)	38x95
Cylinder height, *H*	885
Position of the vortex limiter, *L*	160, 320, 480
Cyclone length, L_1	1,535
Vortex finder insertion length, *S*	*S* = b

advantage of precisely predicting the distribution of static pressure, velocity field, and pressure drop corresponding to the experimental results (Kaya & Karagoz, 2008). On completion of momentum, the QUICK scheme is used (Ansys, 2009; Kaya & Karagoz, 2008). The second-order upwind scheme is used to determine the discretization of kinetic energy and the dissipation rate equation (Shukla, Shukla, & Ghosh, 2011). Discretization of the Reynolds voltage equation is determined using the first-order upwind scheme (Kaya & Karagoz, 2008; Shukla et al., 2011).

To overcome the complexity and flow instability that occurs in a cyclone, a transient simulation with sufficient *time step* is required to model the flow field. The transient simulation is carried out until the static pressure drop stabilizes (Δp = constant) in the *inlet* and *outlet* areas beginning with several iterations of *steady* conditions (Shukla et al., 2011; Sun, Kim, Yang, Kim, & Yoon, 2017). Each numerical simulation performed in this study starts with several steady-state iterations and follows a transient simulation with 2000 *time steps*. The choice of *time step* size is at least one order smaller than the smallest time constant modeled in order to model the transient phenomenon well (ANSY, 2009). The residual time of the fluid in the cyclone is calculated from the dimensions of the cyclone and its flow rate as $t_{res} = Q_{in}/V$ in which Q_{in} is the flow rate at entry and V is the volume of the cyclone (Dirgo & Leith, 1985; Elsayed & Lacor, 2011). The value t_{res} obtained is 0.97–0.99 s so that the *time step* size used in this numerical model is 0.001s. The simulation runs until convergence at any *time step* with an accuracy of 10^{-5} for all variables. Regarding DPM, the maximum number of steps specified is 10^6 and the particle tracking tolerance is limited to 1e-6 (Sun et al., 2017). The combination of *low order* and *high order* schemes is used to complete the movement of particles.

2.3. Boundary conditions and operating conditions

The boundary conditions selected on the *inlet* portion are the *inlet velocity* and *outflow* for the *outlet* and *escape* conditions for each DPM setting. Conditions for the wall boundary are selected on the cyclone wall and lower wall for particle collection. DPM settings for each wall in a sequence are *reflect* and *trap*. Turbulent intensity $I = 0.16(\mathrm{Re}_{Dh})^{-1/8}$is determined on the inlet as well as the hydraulic diameter $D_h = 4A/P$, where A is the cross-sectional area and P is the surrounding wetness (Ansys, 2009). Particle collisions with walls are assumed to be perfectly elastic (e = 1). Table 2 shows the boundary conditions used in this study.

To obtain particle-gathering efficiency, the distribution of particles is injected in the *inlet* portion of the cyclone. The efficiency of particle collection is determined in Equation (18) as follows (Sun et al., 2017):

$$\eta_t = \frac{N_{trapped}}{N_{total}} \times 100 \tag{18}$$

where $N_{trapped}$ is a particle trapped under the *cyclone* and N_{total} is the total number of incoming particles. Various methods are used to present particle size distributions. One is the *Rosin-Rammler* distribution that is used for the *Particle Size Distribution* (PSD) method with the assumption of an exponential relationship between the particle diameter and the fraction of

Table 2. Numeric values of the operating conditions for the simulation

Parameter	Value
Speed at Entry (m/s)	15
Acceleration of Particle Flow (gr/menit)	15
Particle Density (kg/m^3)	1,300
Temperature (K)	288

the particle with a diameter greater than the diameter (d), Y_d as shown in the following Equation (19) (Ansys, 2009):

$$Y_d = e^{\left(\frac{d}{\bar{d}}\right)^n} \tag{19}$$

where d is the particle size (mm), $\bar{d}$ is the average diameter (mm), and n is the dispersion diameter that can be calculated as follows (Ansys, 2009):

$$n = \frac{\ln(-\ln y_d)}{\ln(d/\bar{d})} \tag{20}$$

The particle diameter values in this study ranged from 0.1 μm to 134 with $\bar{d}$ and n as great as 44.4 μm and 1.68 μm, respectively (Safikhani & Mehrabian, 2016).

2.4. Grid generation

The size of the grid used affects the accuracy of a CFD analysis. A smaller grid size yields more accurate results, but it requires significant computing power and takes a longer time compared to larger sized grids. Additionally, to ensure that the results from the selected grid are correct and do not depend on the size and number of elements, simulations based on the number of elements are required. The number of simulated elements is shown in Table 3 along with the error percentage obtained. From Table 3, it can be seen that 514,400 elements produce a lower error value in the experimental results and that increasing the number of elements does not cause a significant error (<5%); therefore, the grid with this number of elements is selected. During simulation, the transient approach regarding with the time simulation set up is used as shown in Table 4. The grid used in this study is a hexahedral grid with 500,000–535,000 elements due to the simulated geometric variation. The result of grid generation is shown in Figure 2.

3. Results and discussion

The three components of speed in the cyclone are tangential speed, axial speed, and radial velocity. Radial velocity, in this case, has little effect over the other velocity components so it can be ignored in the basic calculations (Peng et al., 2002).

The discussion on the effects of the vortex finder diameter and length of vortex limiter on tangential velocity, axial velocity, and static pressure, as well as their effects on particle collection efficiency, will be explained in the next section.

3.1. Validation

The acquisition of numerical simulation results must be verified through validation with experimental data under the same conditions. The results of the simulation in this study were compared

Table 3. Independent *grid* results

Total number of elements	Simulated decreased pressure (Pa)	Experimentally decreased pressure (Pa)	*Error* (%)
376,323	462.64	456.42	1.36
514,400	456.46	456.42	0.01
790,896	451.49	456.42	1.08
980,424	443.28	456.42	2.88

Table 4. Time criteria of the simulation

Time step size (s)	Number of time steps
0.001	2,000

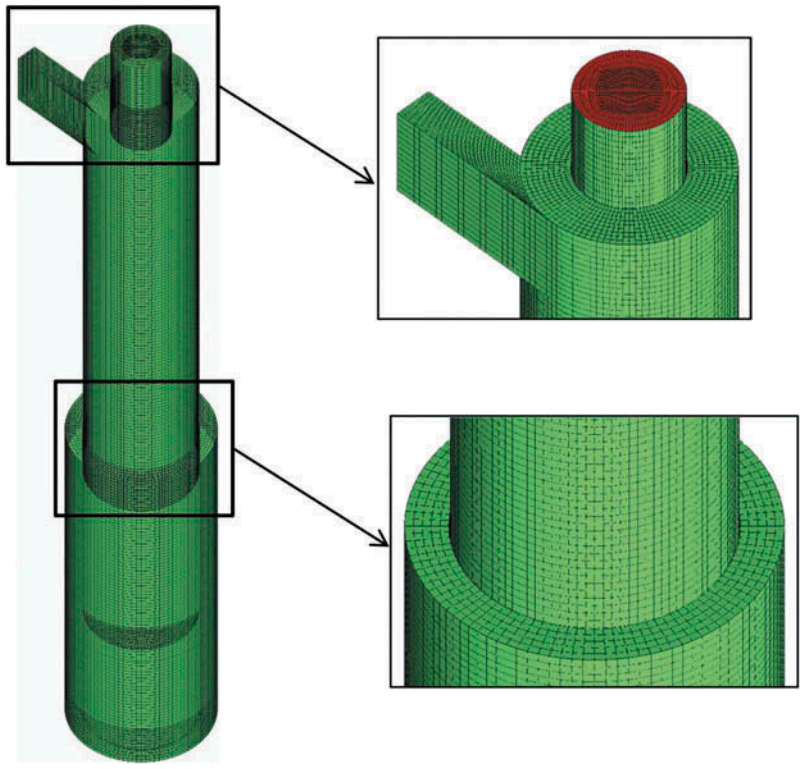

Figure 2. Hexahedral grid generation in the new cylone separator.

with the results of experimental studies conducted by Karagoz et al. (2013). Validation is done by comparing the pressure drop. The pressure drop is obtained from the static pressure difference on the inlet and outlet portions ($\Delta p = p_{in} - p_{out}$). Figure 3 shows that the simulation results are in accordance with the experimental results. However, as the speed increases, the resulting error becomes greater. This is because high velocity causes the flow to become more complex (Safikhani & Mehrabian, 2016).

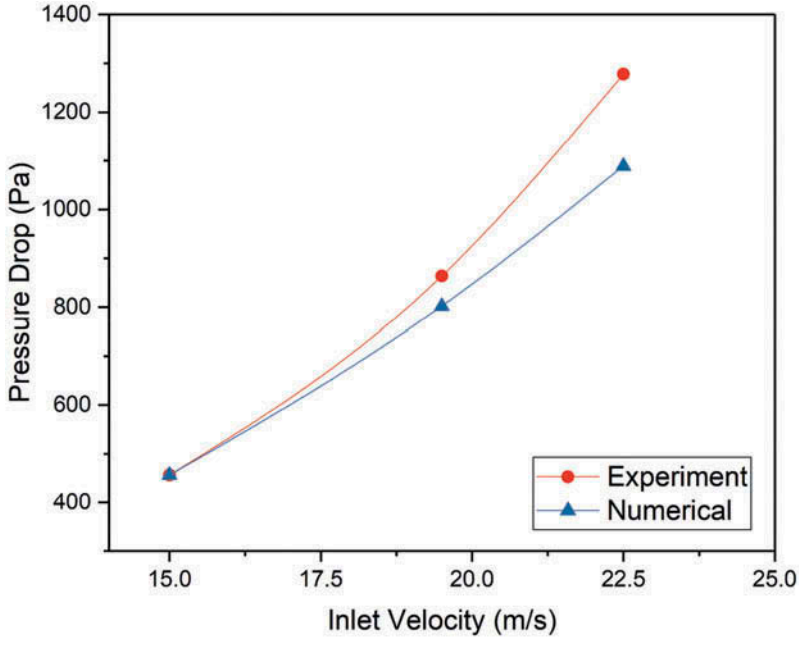

Figure 3. Graphic of the pressure drop results from both the experimental and numerical simulation.

3.2. Effect of tangential speed variation

Tangential velocity is more important than both axial velocity and radial velocity due to the flow caused by high-spinning cyclones. This speed is responsible for much or little particle collection due to the centrifugal force generated. The higher the tangential velocity, the greater the resulting centrifugal force based on this formula $F = mv_\theta^2/r$. The magnitude of the centrifugal force causes the particles to be thrown to the wall and fall downward, thus increasing the collection of particles. As a result, the pressure drop also increases as there is a strong influence between speed and pressure in the cyclone and vice versa for small tangential velocities.

In both Figures 4 and 5 for each modeling of the *new cyclone separator*, there is a *Rankine vortex* as in other *cyclones* where the tangential velocity field is divided into two zones; i.e. inner zone, or quasi vortex flow, surrounded by an outer zone, or quasi-free vortex flow (Hoffman and Stein, 2008; Peng et al., 2002; Safikhani & Mehrabian, 2016). In some simulated cyclones, the tangential velocity has a negative value. This is due to the phenomenon of precessing vortex cores (PVC) resulting in vortex core oscillations on the axis of rotation of cyclone geometry (Brar, Sharma, & Dwivedi, 2014; Cortes & Gil, 2007). This is a common phenomenon found in a cyclone, swirl tube, hydrocyclone, etc. (Brar et al., 2014).

The effects of the vortex finder diameter and length of vortex limiter on tangential velocity are shown in Figures 4 and 5. The tangential velocity affects the velocity of the cyclone core vortex and achieves a maximum value at the boundary between the inner and outer zones of the vortex. It can be seen that by shrinking the vortex finder diameter, the tangential velocity increases. It decreases when the diameter is widened. Regarding the length of the vortex limiter, when the vortex limiter nears the vortex finder, the tangential velocity increases and as the length of the vortex limiter increases, the tangential velocity decreases.

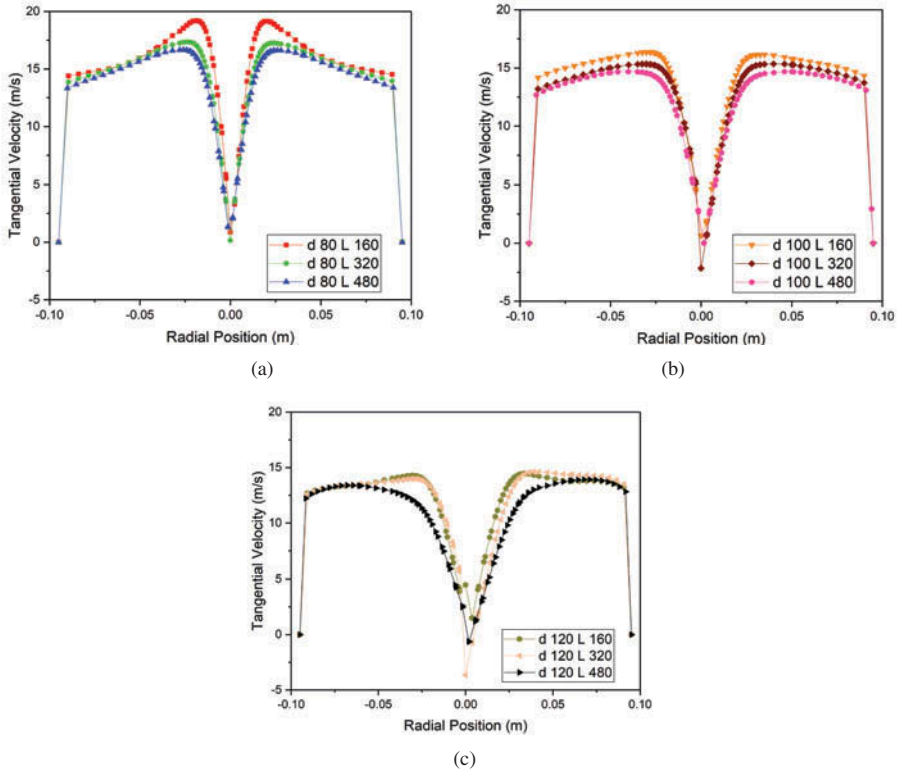

Figure 4. Effects of *vortex limiter* lengths on tangential speed related to the diameter of the *vortex finder* (a) 80 mm, (b) 100 mm, and (c) 120 mm.

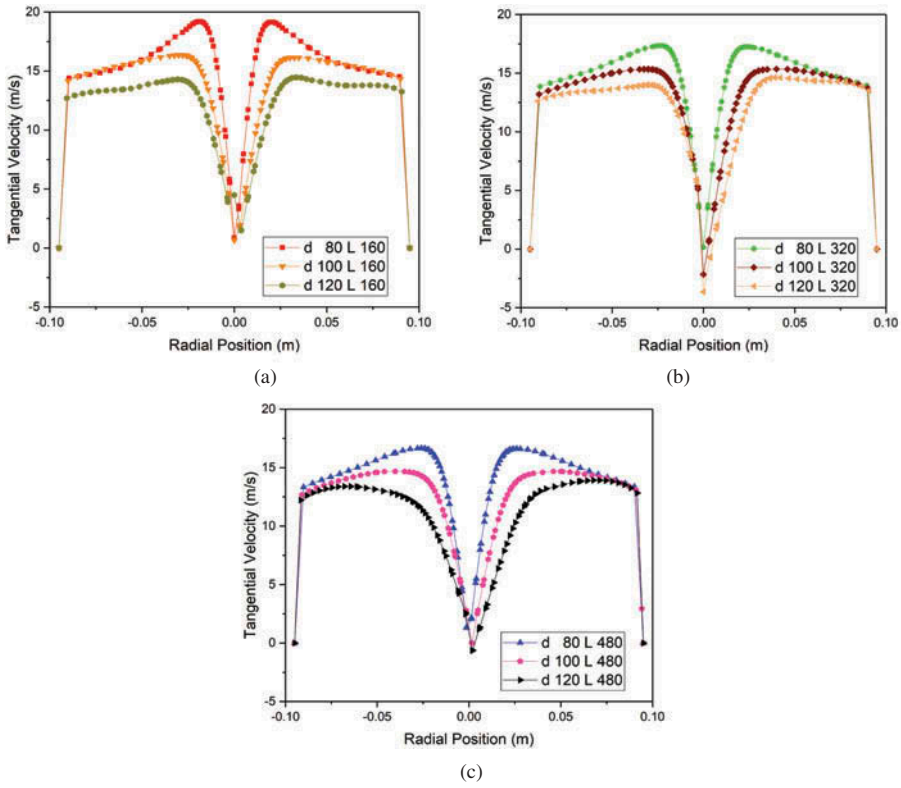

Figure 5. Effects of varying diameters of the *vortex finder* on tangential speed based on lengths of the *vortex limiter* (a) 160 mm, (b) 320 mm, and (c) 480 mm.

3.3. Effect of variation on axial speed

Axial velocity becomes another factor of particle collection because the flow moves both up and down. Figures 6 and 7 show the effect of vortex finder diameter and length of vortex limiter on axial velocity. On the outside of the vortex for each variation, it has a negative axial velocity value that signifies this downward flow so that it has a major influence on bringing the particles to be collected to the bottom of the cyclone (Hoffmann & Stein, 2008). In contrast, a positive axial velocity is useful for bringing particles out through the vortex finder and as the speed decreases, both the diameter of the vortex finder and the length of the vortex limiter increase.

From Figures 6 and 7 we can see that there are two axial velocity profiles: an inverted W profile and a reversed V. This profile gradually changes from an upside-down W to an upside-down V as the vortex finder's diameter diminishes with an increase in the length of its vortex. Inverted W profiles make a maximum axial velocity on the radius of the vortex finder and decrease toward the cyclone core vortex while the inverted V profile creates the maximum axial velocity at the core vortex of the cyclone. This change occurs because the diminution of the vortex finder diameter and the decrease in vortex length causes the core vortex of the cyclone to increase (as indicated by the tangential velocity profile). As a result, the flow can overcome the adverse pressure gradient resulting from the friction forces that arise on the vortex finder walls that weaken the vortex into an inverted V profile (Cortes & Gil, 2007, Elsayed, 2011; Hoekstra, Derksen, & Akker, 1999).

3.4. Influence of variation on static pressure

Figures 8 and 9 show the distributions of static pressure plotted along the axial direction. As the gas enters the cyclone, the gas will follow the geometry of the cyclone's form so that the pressure gradient in the cyclone is dominant in the radial direction. The static pressure reaches the maximum value on the wall area and radially decreases towards the center. In the center

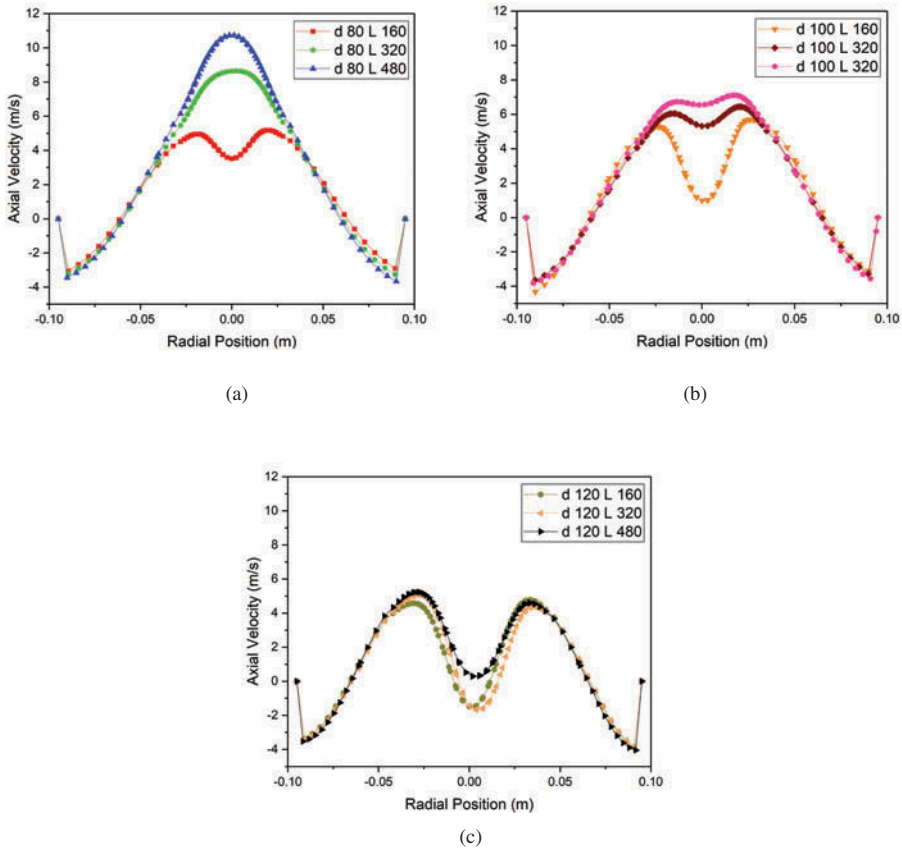

Figure 6. Effects of lengthening the *vortex limiter* on the axial speed based on the diameter of the *vortex finder* (a) 80 mm, (b) 100 mm, and (c) 120 mm.

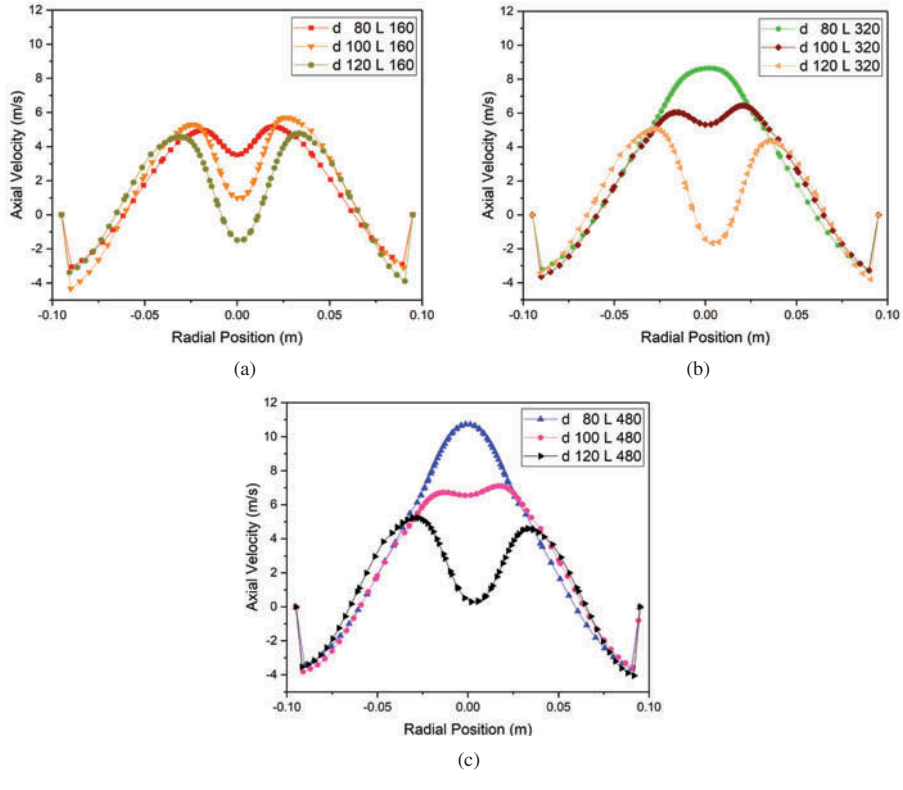

Figure 7. Effects of varying the diameter of the *vortex finder* on the axial speed and the length of the *vortex limiter* (a) 160 mm, (b) 320 mm, and (c) 480 mm.

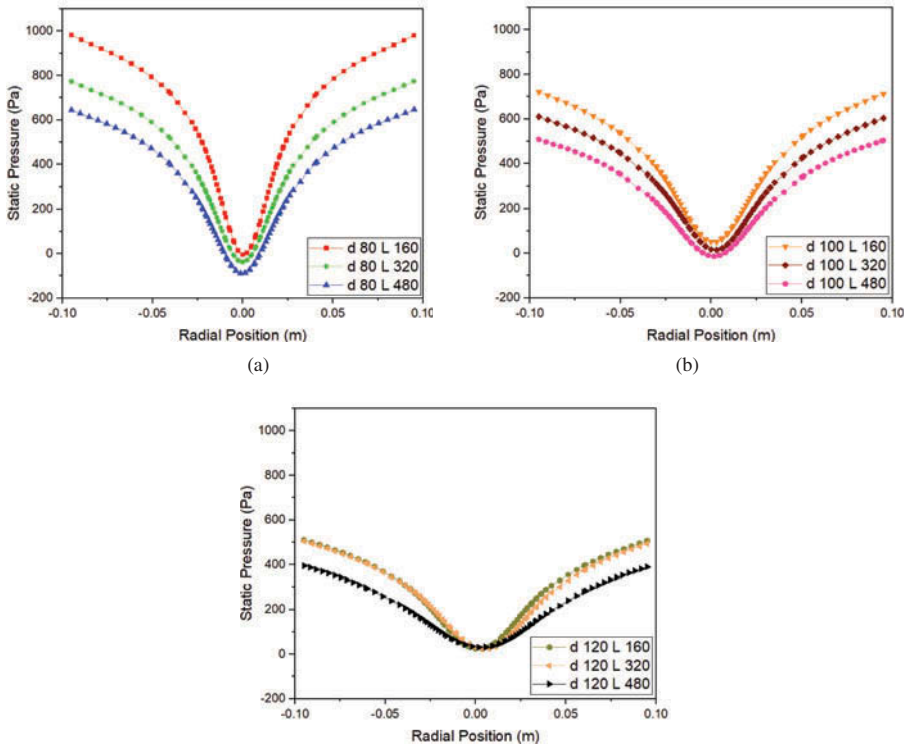

Figure 8. Effects of *vortex limiter* lengths on static pressure based on the diameter of the *vortex finder* (a) 80 mm, (b) 100 mm, and (c) 120 mm.

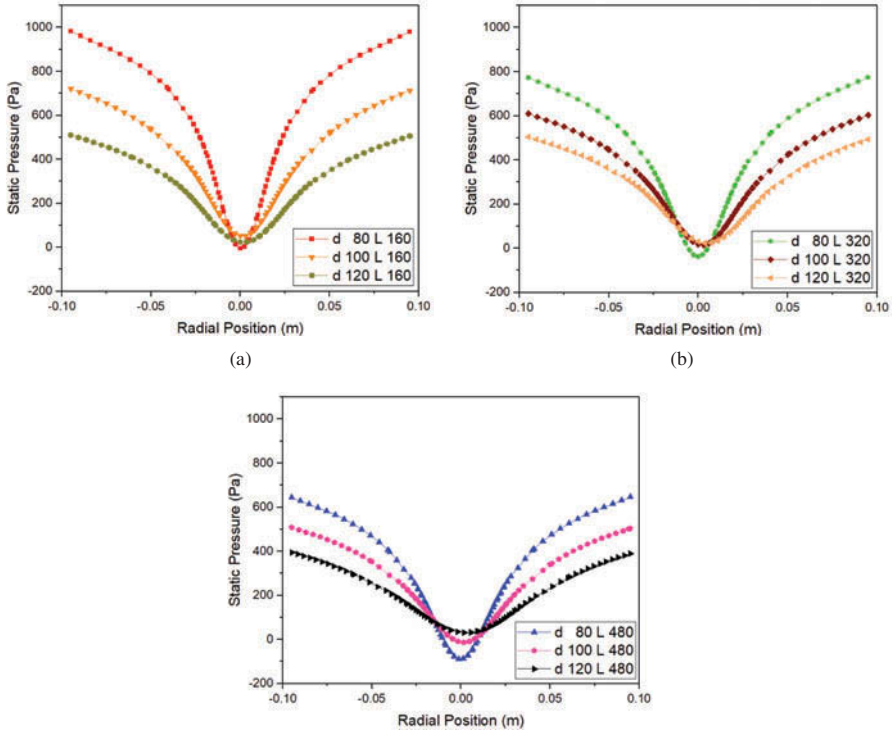

Figure 9. Effects of the varying dimensions of the *vortex finder* on the static pressure based on the length of the *vortex limiter* (a) 160 mm, (b) 320 mm, and (c) 480 mm.

of the cyclone, or in the part of vortex force, appears a static pressure area that has a negative value due to the significantly high rotational speed.

The lowest static pressure lies in the vortex finder with an 80 mm diameter and a 480 mm long vortex limiter. Figure 9 shows that increasing the diameter of the vortex finder causes the gradient pressure toward the wall to decrease and will also dilate the area of low static pressure. The pressure gradient on the wall area increases and there is a reduction of the area of low static pressure when the vortex finder diameter is decreased. The effect of the length of the vortex limiter, as shown in Figure 8, makes the area of low static pressure increase in the axial direction if the vortex limiter is farther away from the vortex finder. This affects the pressure drop due to changes in the size of the diameter of the vortex finder and the length of the occurring vortex so that the pressure drop will decrease as the pressure distribution also decreases.

3.5. Particle collecting efficiency

One of the influences of particle separation is the size of the particle. The particles in the cyclone will split and either exit through the vortex finder or move to the wall area and fall to the bottom of the cyclone. In this study, the effects on particle separation through varying both the vortex finder diameter and the length of the vortex limiter is discussed in the form of particle-gathering efficiency. From Figure 10 it can be seen that the reduced diameter size of the vortex finder gives rise to a high-efficiency collection. Smaller diameters of the vortex finder cause the vortex flow area to forcibly shrink so that the particles exiting the vortex finder will be smaller. In changing the length of the vortex limiter, the efficiency of the collection will increase if the vortex limiter is further away from the vortex finder. Increasing the length of the vortex causes more particles to travel down the cyclone so that more particles accumulate.

4. Conclusion

The numerical simulation in this study used RSM to describe the flow that occurred in the Karagoz *new cyclone separator* based on variations in the diameter of the vortex finder and the length of vortex limiter. Multilevel modeling uses the Eulerian-Lagrangian approach to track particle movements. The tangential velocity, axial velocity, and static pressure obtained from this simulation are analyzed to determine the effect of variations made on the flow field and the efficiency of particle

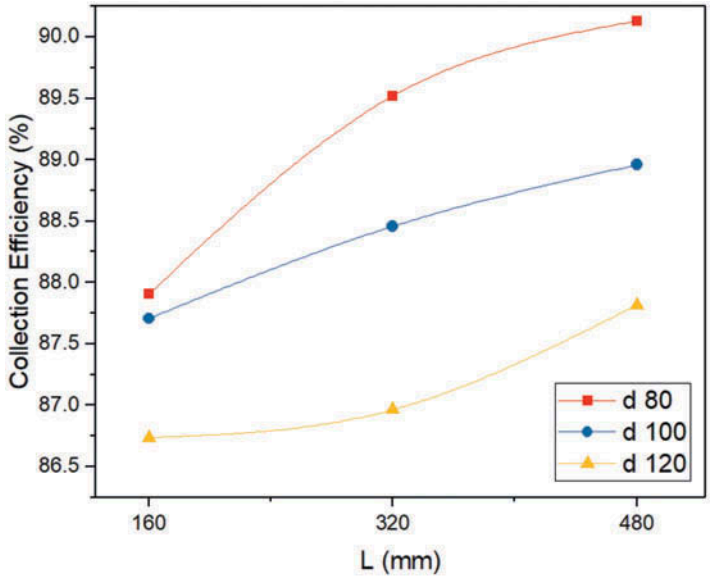

Figure 10. Graphic of collection efficiency.

collection in the new cyclone separator. Based on the simulation results, some conclusions can be drawn as follows:

(1) A decrease in pressure with an increase in both the diameter of the vortex finder and the length of the vortex limiter will decrease as a decreased-value pressure distribution.

(2) Reducing the diameter of the vortex finder boosts collection efficiency by causing an increase in the tangential velocity that generates greater centrifugal force so that the particles are thrown towards the wall and fall down the cyclone.

(3) An increase in the length of the vortex limiter decreases the tangential velocity but increases the collection efficiency because there are fewer separated particles exiting the vortex finder.

Author details
Eflita Yohana[1]
E-mail: efnan2003@gmail.com
Mohammad Tauviqirrahman[1]
E-mail: mohammad.tauviqirrahman@ft.undip.ac.id
E-mail: mtauviq99@yahoo.com
Arbian Ridzka Putra[1]
E-mail: arbianrp@gmail.com
Ade Eva Diana[1]
E-mail: adeeva2010@gmail.com
Kwang-Hwan Choi[2]
E-mail: choikh@pknu.ac.kr
[1] Department of Mechanical Engineering, Diponegoro University, Semarang, Indonesia.
[2] College of Engineering, Pukyong National University, Busan, Korea.

Citation information
Cite this article as: Numerical analysis on the effect of the vortex finder diameter and the length of vortex limiter on the flow field and particle collection in a new cyclone separator, Eflita Yohana, Mohammad Tauviqirrahman, Arbian Ridzka Putra, Ade Eva Diana & Kwang-Hwan Choi, *Cogent Engineering* (2019), 5: 1562319.

References

Alavi, S., Lay, E., & Makhmali, Z. (2018). A CFD study of industrial double-cyclone in HDPE drying process. Engineering Science Journal, 2(1), 31–38. doi:10.28991/esj-2018-01125

ANSYS (2012), ANSYS Help manual, release 14.5, Inc., Pittsburgh, Pennsylvania of USA.

Brar, L. S., Sharma, R. P., & Dwivedi, R. (2014). Effect of vortex finder diameter on flow field and collection efficiency of cyclone separators. Particulate Science and Technology, 33, 34–40. doi:10.1080/02726351.2014.933144

Cortes, C., & Gil, A. (2007). Modeling the gas and particle flow inside cyclone separators. Progress in Energy and Combustion Science, 33, 409–452. doi:10.1016/j.pecs.2007.02.001

Dirgo, J., & Leith, D. (1985). Cyclone collection efficiency: Comparison of experimental results with theoretical predictions. Aerosol Science and Technology, 4(4), 401–415. doi:10.1080/02786828508959066

Elsayed, K. (2011). *Analysis and optimization of cyclone separators geometry using RANS and LES methodologies* (PhD Thesis). Vrije Universiteit Brussel.

Elsayed, K., & Lacor, C. (2011). The effect of cyclone inlet dimensions on the flow pattern and performance. Applied Mathematical Modelling, 35(4), 1952–1968. doi:10.1016/j.apm.2010.11.007

Griffiths, W.D., & Boysan, F. (1996). Computational fluid dynamics (CFD) and empirical modeling of a number of cyclone samplers. *Journal of Aerosol Science, 27* (2), 281–304. doi:10.1016/0021-8502(95)00549-8

Hoekstra, A. J., Derksen, J. J., & Akker, H. E. (1999). An experimental and numerical study of turbulent swirling flow in gas cyclones. Chemical Engineering Science, 54, 2055–2065. doi:10.1016/s0009-2509(98)00373-x

Hoffmann, A., & Stein, L. (2008). Gas cyclones and swirl tubes principles, design, and operation (2nd ed.). Berlin Heidelberg: Springer. doi:10.1007/978-3-540-74696-6

Karagoz, I., Avci, A., Surmen, A., & Sendogan, O. (2013). Design and performance evaluation of a new cyclone separator. Journal of Aerosol Science, 59, 57–64. doi:10.1016/j.jaerosci.2013.01.010

Kaya, F., & Karagoz, I. (2008). Performance analysis of numerical schemes in highly swirling turbulent flows in cyclones. Current Science, 94(10), 1273–1278.

Lim, K. S., Kim, H. S., & Lee, K. W. (2004). Comparative performances of conventional cyclones and a double cyclone with and without an electric field. Journal of Aerosol Science, 35(1), 103–116. doi:10.1016/j.jaerosci.2003.07.001

Morsi, S. A., & Alexander, A. J. (1972). An investigation of particle trajectories in two-phase flow systems. Journal of Fluid Mechanics, 55(2), 193–208. doi:10.1017/s0022112072001806

Peng, W., Hoffmann, A. C., Boot, P. J., Udding, A., Dries, H., Ekker, A., & Kater, J. (2002). Flow pattern in reverse-flow centrifugal separators. Powder Technology, 127(3), 212–222. doi:10.1016/s0032-5910(02)00148-1

Safikhani, H., & Mehrabian, P. (2016). Numerical study of flow field in new cyclone separators. Advanced Powder Technology, 27(2), 379–387. doi:10.1016/j.apt.2016.01.011

Shukla, S. K., Shukla, P., & Ghosh, P. (2011). Evaluation of numerical schemes using different simulation methods for the continuous phase modeling of cyclone separators. Advanced Powder Technology, 22(2), 209–219. doi:10.1016/j.apt.2010.11.009

Song, C., Pei, B., Jiang, M., Wang, B., Xu, D., & Chen, Y. (2016). Numerical analysis of forces exerted on particles in cyclone separators. Powder Technology, 294, 437–448. doi:10.1016/j.powtec.2016.02.052

Sun, X., Kim, S., Yang, S. D., Kim, H. S., & Yoon, J. Y. (2017). Multi-objective optimization of a Stairmand cyclone separator using response surface methodology and computational fluid dynamics. Powder Technology, 320, 51–65. doi:10.1016/j.powtec.2017.06.065

Xiang, R. B., & Lee, K. W. (2001). Exploratory study on cyclones of modified designs. Particulate Science and Technology, 19(4), 327–338. doi:10.1080/02726350290057868

Zhao, B., Su, Y., & Zhang, J. (2006). Simulation of gas flow pattern and separation efficiency in cyclone with conventional single and spiral double inlet configuration. Chemical Engineering Research and Design, 84(12), 1158–1165. doi:10.1205/cherd06040

Zhu, Y., Kim, M. C., Lee, K. W., Park, Y. O., & Kuhlman, M. R. (2001). Design and performance evaluation of a novel double cyclone. Aerosol Science and Technology, 34(4), 373–380. doi:10.1080/02786820120723

Cogent Engineering **(ISSN: 2331-1916) is published by Cogent OA, part of Taylor & Francis Group.**

Publishing with Cogent OA ensures:

- Immediate, universal access to your article on publication
- High visibility and discoverability via the Cogent OA website as well as Taylor & Francis Online
- Download and citation statistics for your article
- Rapid online publication
- Input from, and dialog with, expert editors and editorial boards
- Retention of full copyright of your article
- Guaranteed legacy preservation of your article
- Discounts and waivers for authors in developing regions

Submit your manuscript to a Cogent OA journal at www.CogentOA.com